

## Diameter dependence of carbon nanotube thermal conductivity and extension to the graphene limit

L. Lindsay,<sup>1,2</sup> D. A. Broido,<sup>1</sup> and Natalio Mingo<sup>3,4</sup>

<sup>1</sup>*Department of Physics, Boston College, Chestnut Hill, Massachusetts 02467, USA*

<sup>2</sup>*Department of Physics, Computer Science and Engineering, Christopher Newport University, Newport News, Virginia 23606, USA*

<sup>3</sup>*CEA-Grenoble, 17 Rue des Martyrs, Grenoble 38000, France*

<sup>4</sup>*Department of Electrical Engineering, University of California, Santa Cruz, California 95064, USA*

(Received 18 July 2010; revised manuscript received 16 September 2010; published 5 October 2010)

Using an exact numerical solution of the phonon Boltzmann equation, we demonstrate a nontrivial evolution with diameter of the intrinsic lattice thermal conductivity,  $\kappa$ , of a wide range of achiral and chiral single-walled carbon nanotubes (SWCNTs) into that of graphene,  $\kappa_{\text{graphene}}$ . We find that  $\kappa < \kappa_{\text{graphene}}$  for all but the smallest diameter SWCNTs and that  $\kappa$  exhibits a minimum for modest diameters. This behavior results because the inherent curvature in SWCNTs violates a selection rule in graphene arising from its reflection symmetry, which strongly restricts phonon-phonon scattering in that system.

DOI: [10.1103/PhysRevB.82.161402](https://doi.org/10.1103/PhysRevB.82.161402)

PACS number(s): 66.70.-f, 63.20.kg, 63.22.Gh, 63.22.Rc

### I. INTRODUCTION

Graphene and single-walled carbon nanotubes (SWCNTs) have attracted intense interest in recent years, in part because of the broad array of fascinating electronic and transport properties that they have exhibited.<sup>1-7</sup> These two systems are closely related: SWCNTs can be viewed as graphene strips rolled into cylinders of various diameters and chiralities. For very large diameters, the material properties of SWCNTs should, in principle, approach those of graphene. Yet, the vast number of carbon atoms that need to be included in theoretical models of large diameter SWCNTs make it a significant computational challenge to investigate this limit.

In this Rapid Communication, we describe how the graphene limit is achieved in the context of phonon thermal transport. We have developed an efficient Boltzmann transport equation (BTE) approach to calculate the intrinsic lattice thermal conductivity,  $\kappa$ , of SWCNTs.<sup>8</sup> This approach includes the commonly ignored<sup>9,10</sup> optic modes, which we find are essential in accurately describing phonon transport in SWCNTs. We have also developed an analogous approach<sup>6,11</sup> for the thermal conductivity of graphene,  $\kappa_{\text{graphene}}$ . Our investigation has elucidated the following remarkable features: (1) for the wide range of achiral and chiral SWCNTs considered,  $\kappa < \kappa_{\text{graphene}}$  except at very small diameters; (2)  $\kappa$  exhibits a minimum at modest SWCNT diameters; (3)  $\kappa \rightarrow \kappa_{\text{graphene}}$  from below for large diameter SWCNTs. This unexpected behavior is explained through a symmetry-based selection rule in graphene<sup>6,11</sup> that strongly restricts the phonon-phonon scattering in that system. The inherent curvature of SWCNTs breaks this selection rule causing enhanced phonon-phonon scattering and decreasing  $\kappa$  compared to  $\kappa_{\text{graphene}}$ .

### II. PHONON-PHONON SCATTERING SELECTION RULES IN SWCNTs AND GRAPHENE

We consider a graphene sheet in the  $x$ - $y$  plane having infinite width and length,  $L$ . Achiral and chiral SWCNTs are also taken to be of length,  $L$ , and with diameter,  $d$ . We take a

two-atom unit cell for both graphene and SWCNTs.<sup>12,13</sup> The phonon modes in each system are then specified by three quantum numbers  $\lambda=(j, \mathbf{q})$ , where  $j=1, \dots, 6$  and  $\mathbf{q}$  is the phonon momentum. In graphene,  $\mathbf{q}=(q_x, q_y)$  is a two-dimensional wave vector, associated with the translational symmetry of the hexagonal lattice. The phonon spectrum consists of three “acoustic” branches and three optic branches. The transverse-acoustic (TA) and longitudinal-acoustic (LA) branches correspond to in-plane atomic vibrations with  $\omega \sim q$  for  $q \rightarrow 0$ . The out-of-plane or flexure modes are designated by the letter “Z.” The flexure-acoustic branch (ZA) has  $\omega \sim q^2$  as  $q \rightarrow 0$ . For  $(n_1, n_2)$  SWCNTs,  $\mathbf{q}=(q, l)$ , where  $q$  is the wave number along the nanotube axis,  $-\pi < q \leq \pi$ , and the angular quantum number,  $l$ , takes on the integral values  $l=0, \pm 1, \dots, +g/2$ , where  $g$  is the number of two-atom unit cells in the translational unit cell of the SWCNT (Ref. 14) and reduces to  $2n$  for the achiral  $(n, 0)$  and  $(n, n)$  SWCNTs. The vibrational modes consist of linear torsional and longitudinal-acoustic branches, two quadratic flexure branches, and  $6g-4$  optic branches.

For defect-free SWCNTs and graphene, anharmonic three-phonon scattering provides the thermal resistance that limits  $\kappa$  and  $\kappa_{\text{graphene}}$ . Conservation of phonon momentum and energy requires:<sup>6,8,11</sup>  $\mathbf{q} \pm \mathbf{q}' = \mathbf{q}'' + \mathbf{G}$  and  $\omega_\lambda \pm \omega_{\lambda'} = \omega_{\lambda''}$ , where  $\omega_\lambda$  is the frequency of phonon mode  $\lambda$  and  $\mathbf{G}$  is a reciprocal-lattice vector with  $\mathbf{G}=0$  for normal ( $N$ ) processes and  $\mathbf{G} \neq 0$  for umklapp ( $U$ ) processes. In graphene,  $\mathbf{G} = m_1 \mathbf{b}_1 + m_2 \mathbf{b}_2$ , where  $\mathbf{b}_{1,2} = 2\pi(1/\sqrt{3}, \pm 1)$ , and  $m_1$  and  $m_2$  are integers. In chiral and achiral SWCNTs the momentum selection rule is more complex:<sup>7,15</sup>  $q \pm q' = q'' + G$ ,  $l \pm l' = (l'' + l_G) \text{ mod}[g]$ . Here, the mod function keeps  $l'' + l_G$  between  $-g/2 + 1$  and  $g/2$ . For  $N$  scattering processes,  $G = l_G = 0$ . For  $U$  scattering processes,  $G = \pm 2\pi$  and the integer  $l_G = \pm p$ , where  $p$  is an integer such that, for chiral SWCNTs,  $p > n_{>}$ , where  $n_{>}$  is the larger of  $n_1$  and  $n_2$ , and for achiral SWCNTs  $p = n$ .<sup>7,15</sup> Thus, since the acoustic modes can only have  $l=0, \pm 1$ , the  $l$  selection rule requires that  $U$  processes involve at least one optic mode for SWCNTs with  $n$  or  $n_{>} \geq 4$ ; this includes all SWCNTs of practical interest. This point has been missed in previous models, which did not use

the correct  $l$  selection rule.<sup>16,17</sup> A number of models have simply ignored the optic modes altogether.<sup>9,10</sup>

In graphene, reflection symmetry leads to another important selection rule:<sup>6,11</sup> *for the anharmonic phonon-phonon interaction, out-of-plane phonon modes only scatter in pairs.* This selection rule strongly restricts the phase space for phonon-phonon scattering. In principle, it does not hold in SWCNTs because of their curvature. However, we will show that it becomes important for large  $d$  SWCNTs whose curvature is small.<sup>18</sup>

### III. PHONON THERMAL TRANSPORT

We implement here an exact numerical solution to the phonon BTE for SWCNTs (Ref. 8) and graphene.<sup>6,11</sup> This approach includes the inelastic three-phonon scattering processes responsible for the intrinsic thermal resistance as well as boundary scattering that occurs because of the finite sample lengths,  $L$ . The linearized phonon BTE can be expressed in terms of a set of coupled equations for the phonon lifetimes,  $\tau_\lambda$ ,<sup>19</sup>

$$\tau_\lambda = \tau_\lambda^0(1 + \Delta_\lambda), \quad (1)$$

where  $1/\tau_\lambda^0 \equiv \Sigma_{(+)}\Gamma_{\lambda\lambda'\lambda''}^{(+)} + 1/2\Sigma_{(-)}\Gamma_{\lambda\lambda'\lambda''}^{(-)} + 1/\tau_\lambda^{bs}$  defines  $\tau_\lambda^0$ , the phonon lifetime in the relaxation-time approximation (RTA), and the (+) and (-) denote sums over  $\lambda', \lambda''$  for the two different types of three-phonon processes  $\lambda \pm \lambda' \leftrightarrow \lambda''$ , which extend over the numerically determined energy and momentum-conserving phase space of  $N$  and  $U$  processes. For each  $\mathbf{q}$  and triplet of phonon branches ( $j, j', j''$ ) involved, this phase space is comprised of distinct points (SWCNTs) or curve segments (graphene) in the two-dimensional space of  $\mathbf{q}'$ . The term,  $\tau_\lambda^{bs} = L/2|v_\lambda|$  is a boundary scattering time with  $v_\lambda$  being the phonon velocity component in the transport direction. This form correctly recovers the ballistic ( $L \rightarrow 0$ ) and diffusive ( $L \rightarrow \infty$ ) limits.<sup>20</sup> The terms,  $\Gamma_{\lambda\lambda'\lambda''}^{(\pm)} = W_{\lambda\lambda'\lambda''}^{(\pm)}/n_\lambda^0(n_\lambda^0 + 1)$ , where  $n_\lambda^0$  is the Bose factor and the  $W_{\lambda\lambda'\lambda''}^{(\pm)}$  are the three-phonon scattering rates defined previously;<sup>6,8,11</sup> these contain the third-order interatomic force constants, and the phonon frequencies and eigenvectors. These latter quantities are determined using derivatives of an optimized Tersoff empirical interatomic potential,<sup>21,22</sup> which has been minimized<sup>23</sup> to obtain the lattice constant, for each case considered.

The three-phonon scattering processes are inelastic. This is reflected by the presence of the term,  $\Delta_\lambda$  in Eq. (1), where

$$\Delta_\lambda = \sum_{\lambda'\lambda''}^{(+)}\Gamma_{\lambda\lambda'\lambda''}^{(+)}(\xi_{\lambda\lambda''}\tau_{\lambda''} - \xi_{\lambda\lambda'}\tau_{\lambda'}) + \frac{1}{2}\sum_{\lambda'\lambda''}^{(-)}\Gamma_{\lambda\lambda'\lambda''}^{(-)}(\xi_{\lambda\lambda''}\tau_{\lambda''} + \xi_{\lambda\lambda'}\tau_{\lambda'}), \quad (2)$$

where  $\xi_{\lambda\lambda'} = v_\lambda \omega_\lambda / v_{\lambda'} \omega_{\lambda'}$ . The term,  $\Delta_\lambda$ , couples out-of-equilibrium phonons in each mode  $\lambda$  to phonons in other modes ( $\lambda', \lambda''$ ) subject to the energy and momentum conservation conditions. Neglect of  $\Delta_\lambda$  is equivalent to a RTA with relaxation time  $\tau_\lambda^0$ . For systems with strong  $U$  scattering, first-principles calculations<sup>24</sup> have shown the RTA to work well. However, for SWCNTs and graphene,  $N$  three-phonon

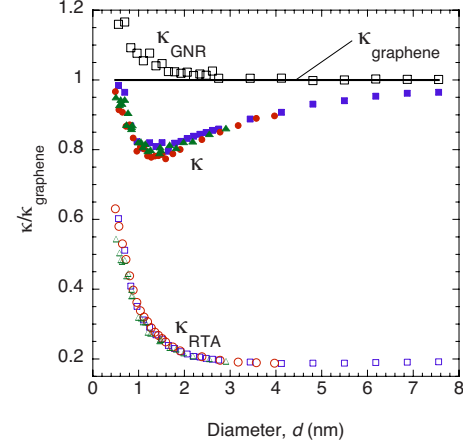


FIG. 1. (Color online)  $\kappa$  vs  $d$  for a variety of zigzag (solid red circles), armchair (solid blue squares), and chiral (solid green triangles) SWCNTs. The black line shows  $\kappa_{\text{graphene}}$  while the black open squares give  $\kappa_{\text{GNR}}$ . Open red circles, blue squares, and green triangles are RTA results for zigzag, armchair, and chiral SWCNTs. For all cases,  $L=3 \mu\text{m}$  and  $T=300 \text{ K}$ . All values are scaled by  $\kappa_{\text{graphene}}$ .

scattering contributions are particularly important and  $U$  scattering is relatively weak,<sup>6,8,11</sup> so inclusion of  $\Delta_\lambda$  is essential to accurately describe phonon thermal transport.

The coupled equations for  $\tau_\lambda$  are solved using an iterative scheme<sup>6,8,11</sup> and  $\kappa$ , is calculated as

$$\kappa = \begin{cases} \frac{1}{2\pi^2 d \delta} \sum_{j,l} \int (\partial n^0 / \partial T) \hbar \omega_{jl}(\mathbf{q}) v_{jl}^2(\mathbf{q}) \tau_{jl}(\mathbf{q}) d\mathbf{q} & \text{SWCNTs} \\ \frac{1}{4\pi^2 \delta} \sum_j (\partial n^0 / \partial T) \hbar \omega_j(\mathbf{q}) v_j^2(\mathbf{q}) \tau_j(\mathbf{q}) d\mathbf{q} & \text{graphene}, \end{cases} \quad (3)$$

where  $\delta=0.335 \text{ nm}$  is the separation between the carbon planes in graphite. Since  $\kappa_{\text{graphene}}$  is isotropic,<sup>25</sup> we only consider transport in the armchair direction for graphene.<sup>26</sup>

### IV. RESULTS AND DISCUSSION

Our efficient BTE approach has made possible calculations of  $\kappa$  in a wide variety of SWCNTs, which have not been previously explored theoretically with  $d$  ranging from 0.42 to 7.56 nm. We have considered 24 armchair SWCNTs ranging in size from (4,4) to (55,55). We have also considered 22 zigzag SWCNTs from (6,0) to (50,0) and 25 chiral SWCNTs ranging from (6,3) to (32,8). To highlight the computational challenges posed by the large diameter SWCNTs, we note that the (55,55) SWCNT has 660 phonon branches, and about 120 million  $N$  and  $U$  three-phonon processes are included in the calculation of  $\kappa$ . For all SWCNTs, we find that the optic modes provide significant contributions to  $\kappa$  which increase with  $d$ .

Figure 1 plots  $\kappa$  vs  $d$  for length,  $L=3 \mu\text{m}$ , and at  $T=300 \text{ K}$ . All values have been scaled to the calculated  $\kappa_{\text{graphene}}=2436 \text{ W m}^{-1} \text{ K}^{-1}$  for the same  $L$  and  $T$ , indicated by the solid black line. Since the diameters of armchair

SWCNTs are larger than the corresponding zigzag SWCNTs by a factor of  $\sqrt{3}$  for the same number of atoms per translational unit cell, we are able to extend the armchair results further. For reference, the commonly studied (10,0) and (10,10) SWCNTs have  $d=0.8$  nm and  $d=1.4$  nm, respectively. Chiral SWCNTs have very large translational unit cells even for relatively small  $d$  and thus cannot be extended as far as the achiral SWCNTs.

Also shown in Fig. 1 are the calculated thermal conductivities,  $\kappa_{\text{GNR}}$ , of armchair graphene nanoribbons (GNRs) of length,  $L=3$   $\mu\text{m}$ . Artificial periodic boundary conditions at the right and left GNR edges are used so that GNRs of width,  $W$ , correspond to armchair SWCNTs with  $d=W/\pi$ . Thus, the difference between  $\kappa$  and  $\kappa_{\text{GNR}}$  is due solely to the curvature of the SWCNTs. For large  $d$ ,  $\kappa_{\text{GNR}}=\kappa_{\text{graphene}}$ . As  $d$  decreases, so does the number of phonon modes, but because many optic modes are pushed to higher frequencies, they can only weakly scatter the lower frequency heat-carrying phonon modes. This causes  $\kappa_{\text{GNR}}$  to eventually rise above  $\kappa_{\text{graphene}}$ . We note that the graphene selection rule still holds for GNRs.

The behavior of  $\kappa$  for SWCNTs is quite different. For large  $d$ ,  $\kappa\approx\kappa_{\text{graphene}}$ . However, as  $d$  decreases,  $\kappa$  is reduced. This reduction occurs because of the enhanced phonon-phonon scattering arising from the breaking of the graphene selection rule with increasing SWCNT curvature. At  $d\equiv d_{\text{min}}\sim 1.5$  nm, a minimum in  $\kappa$  forms. This reflects a competition between the increasingly violated selection rule and the removal of phonon-phonon scattering channels as in the case of GNRs. With further decrease in  $d$ , the latter effect wins out and  $\kappa$  rises such that  $\kappa\sim\kappa_{\text{graphene}}$  for the smallest diameter SWCNTs considered.

We have also calculated the ballistic thermal conductivity of armchair SWCNTs,  $\kappa_{\text{ballistic}}$  vs  $d$  (not shown), obtained by turning off phonon-phonon scattering. We find that by the  $d=d_{\text{min}}$  for  $\kappa$ ,  $\kappa_{\text{ballistic}}$  is already 97% of the corresponding ballistic graphene value of  $12\,800\text{ W m}^{-1}\text{ K}^{-1}$ . Since  $\kappa_{\text{ballistic}}$  involves only phonon mode frequencies and velocities, this means that by this value of  $d$ , SWCNT dispersions are matching those of graphene. Furthermore,  $\kappa_{\text{ballistic}}\gg\kappa$  so that phonon-phonon scattering already provides the majority of thermal resistance at  $L=3$   $\mu\text{m}$ . This corroborates that the observed reduction in  $\kappa$  compared to  $\kappa_{\text{graphene}}$  stems from enhanced phonon-phonon scattering through the breaking of the graphene selection rule.

To further elucidate the large  $d$  behavior of  $\kappa$ , Fig. 2 shows the contributions,  $\kappa_j$ , to  $\kappa$  for each  $j=1, 2, \text{ and } 3$  [obtained by summing over the  $2n\ l$  values in Eq. (3)], for armchair SWCNTs (small circles) compared to the corresponding contributions to  $\kappa_{\text{graphene}}$  (horizontal lines). For large  $d$ , the  $\kappa_j$  for  $j=1, 2, \text{ and } 3$  merge with their ZA, TA, and LA graphene counterparts. Note that the ZA branch provides the majority of the contribution to  $\kappa_{\text{graphene}}$ . We have previously found<sup>6,11</sup> that this occurs because of the graphene selection rule and the dominance of the  $N$  compared to  $U$  phonon-phonon scattering rates arising from the large ZA phonon density of states at small  $\omega$ . Furthermore, while  $\kappa_2$  and  $\kappa_3$  have converged to the TA and LA values by  $d\sim 3$  nm,  $\kappa_1$  continues to gradually increase, tracking the rise in the total  $\kappa$ . Since by its nature, the graphene selection rule

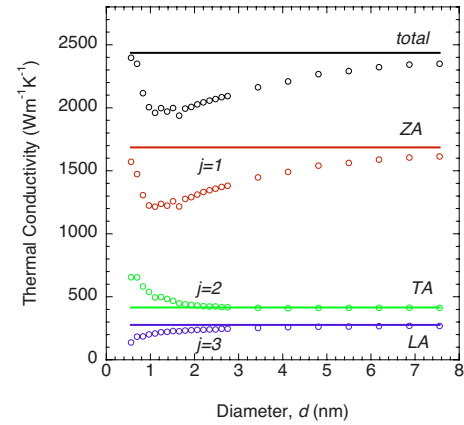


FIG. 2. (Color online) Contributions to  $\kappa$  summed over  $l$ , for each  $j$  vs  $d$  for armchair SWCNTs with  $L=3$   $\mu\text{m}$  at  $T=300$  K.  $j=1, 2, \text{ and } 3$  and total correspond to red, green, blue, and black circles, respectively. The horizontal lines show the associated contributions to  $\kappa_{\text{graphene}}$  for the ZA, TA, and LA modes as well as the total.

most strongly affects the ZA phonons the observed rise in  $\kappa$  for large  $d$  is a consequence of the onset of this selection rule. We have found previously<sup>6,11</sup> that the graphene selection rule forbids about 60% of the three-phonon-scattering phase space that would otherwise be allowed from momentum and energy conservation. Thus, for large diameter SWCNTs, the strengths of a huge number of such scattering processes decrease resulting in the observed increase in  $\kappa$ .

Although corrections have been devised,<sup>27</sup> in the conventional RTA,  $N$  scattering processes are purely resistive. Thus, the increased  $N$  scattering with diameter noted above should lower  $\kappa_{\text{RTA}}$ . This unphysical behavior is seen in Fig. 1 by the lower set of symbols, which shows the RTA thermal conductivity of SWCNTs obtained by using  $\tau_{\lambda}^0$  instead of  $\tau_{\lambda}$  in Eq. (3). In real systems, the momentum conserving  $N$  processes cannot themselves provide thermal resistance but instead affect  $\kappa$  indirectly by redistributing phonons to larger wave vectors where  $U$  scattering can take place. Thus, if only  $N$  processes were present, the  $\kappa$  of a perfect infinite crystal would diverge. Such unusual behavior is typically seen only at very low temperatures in most materials but manifests itself in large diameter SWCNTs and graphene even at room and higher temperatures. This highlights the importance of using a full solution of the phonon BTE in SWCNTs and graphene rather than the commonly used RTA approach.

We cannot make direct comparison with measured  $\kappa$  values for SWCNTs since there are only a few such measurements and the diameters are not accurately obtained.<sup>2,3</sup> However, we note that the measured  $\kappa$  values for SWCNTs (Refs. 2 and 3) and graphene,<sup>5</sup> while they extend over a wide range, are consistently higher than our calculated results. This may arise from a too strong anharmonicity expressed in the optimized Tersoff potential,<sup>22</sup> a possibility borne out by the calculated temperature dependence of  $\kappa$  for SWCNTs (not shown) and graphene. The calculated peaks in  $\kappa(T)$  as well as the per branch contributions are relatively insensitive to diameter and occur at about the same peak location ( $T\sim 175$  K) as for  $\kappa_{\text{graphene}}$ .<sup>6</sup> However, this is below the mea-

sured peak for SWCNTs ( $T \sim 300$  K),<sup>3</sup> suggesting that three-phonon scattering is too strong. We note that any improved representation of the anharmonicity should not change the qualitative diameter dependence shown in Fig. 1 but it may, e.g., increase the range of small  $d$  values where  $\kappa > \kappa_{\text{graphene}}$ .

We note that previous calculations<sup>28,29</sup> corroborate qualitatively the monotonic decrease in  $\kappa$  with  $d$  seen in Fig. 1 for small to moderate  $d$ . Reference 29 obtains  $\kappa > \kappa_{\text{graphene}}$ , contrary to our finding. However, the obtained  $\kappa_{\text{graphene}}$  in Ref. 29 is almost an order of magnitude below ours so it is difficult to make a direct comparison with this work.

## V. CONCLUSIONS

We have calculated  $\kappa$  for a wide diameter range of achiral and chiral SWCNTs using a full solution of the phonon BTE.

We find that, for all but the smallest  $d$ ,  $\kappa < \kappa_{\text{graphene}}$  and it exhibits a nontrivial dependence on  $d$ , displaying a minimum for  $d$  of a few nanometers; in contrast  $\kappa_{\text{GNR}} \geq \kappa_{\text{graphene}}$  and decreases monotonically with increasing  $d$ . This behavior is connected to a symmetry-based selection rule on phonon-phonon scattering in graphene and the GNRs, which is violated in SWCNTs because of their curvature.

## ACKNOWLEDGMENTS

The authors gratefully acknowledge the National Science Foundation for support of this research under Grants No. CBET 0651381 and No. 0651310. N.M. acknowledges support from the French “Agence Nationale de la Recherche.”

- 
- <sup>1</sup>K. S. Novoselov, A. K. Geim, S. V. Morozov, D. Jiang, Y. Zhang, S. V. Dubonos, I. V. Grigorieva, and A. A. Firsov, *Science* **306**, 666 (2004).
- <sup>2</sup>C. Yu, L. Shi, Z. Yao, D. Li, and A. Majumdar, *Nano Lett.* **5**, 1842 (2005).
- <sup>3</sup>E. Pop, D. Mann, Q. Wang, K. Goodson, and H. Dai, *Nano Lett.* **6**, 96 (2006).
- <sup>4</sup>N. Hamada, A. Sawada, and A. Oshiyama, *Phys. Rev. Lett.* **68**, 1579 (1992).
- <sup>5</sup>A. A. Balandin, S. Ghosh, W. Bao, I. Calizo, D. Teweldebrhan, F. Miao, and C. N. Lau, *Nano Lett.* **8**, 902 (2008).
- <sup>6</sup>J. H. Seol, I. Jo, A. L. Moore, L. Lindsay, Z. H. Aitken, M. T. Pettes, X. Li, Z. Yao, R. Huang, D. A. Broido, N. Mingo, R. S. Ruoff, and L. Shi, *Science* **328**, 213 (2010).
- <sup>7</sup>S. Reich, C. Thomsen, and J. Maultzsch, *Carbon Nanotubes: Basic Concepts and Physical Properties* (Wiley-VCH, Weinheim, 2004).
- <sup>8</sup>L. Lindsay, D. A. Broido, and N. Mingo, *Phys. Rev. B* **80**, 125407 (2009).
- <sup>9</sup>J. X. Cao, X. H. Yan, Y. Xiao, and J. W. Ding, *Phys. Rev. B* **69**, 073407 (2004).
- <sup>10</sup>J. Wang and J.-S. Wang, *Appl. Phys. Lett.* **88**, 111909 (2006).
- <sup>11</sup>L. Lindsay, D. A. Broido, and N. Mingo, *Phys. Rev. B* **82**, 115427 (2010).
- <sup>12</sup>C. T. White, D. H. Robertson, and J. W. Mintmire, *Phys. Rev. B* **47**, 5485 (1993).
- <sup>13</sup>V. N. Popov, V. E. Van Doren, and M. Balkanski, *Phys. Rev. B* **61**, 3078 (2000).
- <sup>14</sup>R. A. Jishi, M. S. Dresselhaus, and G. Dresselhaus, *Phys. Rev. B* **47**, 16671 (1993).
- <sup>15</sup>N. Bozovic, I. Bozovic, and M. Damnjanovic, *J. Phys. A* **18**, 923 (1985); M. Damnjanovic, I. Bozovic, and N. Bozovic, *ibid.* **17**, 747 (1984).
- <sup>16</sup>S. P. Hepplestone and G. P. Srivastava, *Phys. Rev. B* **74**, 165420 (2006).
- <sup>17</sup>Y. Gu and Y. Chen, *Phys. Rev. B* **76**, 134110 (2007).
- <sup>18</sup>We note that the graphene selection rule does not emerge from the widely used long-wavelength approximation to the three-phonon-scattering rates such as employed in Refs. 9, 10, 16, and 17.
- <sup>19</sup>The form of the BTE presented here is equivalent to that in Refs. 6, 8, and 9.
- <sup>20</sup>N. Mingo and D. A. Broido, *Nano Lett.* **5**, 1221 (2005).
- <sup>21</sup>J. Tersoff, *Phys. Rev. Lett.* **61**, 2879 (1988).
- <sup>22</sup>L. Lindsay and D. A. Broido, *Phys. Rev. B* **81**, 205441 (2010).
- <sup>23</sup>In the minimization, the systems are taken to have infinite length; edge effects are not included.
- <sup>24</sup>A. Ward and D. A. Broido, *Phys. Rev. B* **81**, 085205 (2010).
- <sup>25</sup>J. F. Nye, *Physical Properties of Crystals: Their Representation by Tensors and Matrices* (Clarendon Press, Oxford, 1957).
- <sup>26</sup>A small anisotropy in  $\kappa_{\text{graphene}}$  is found in armchair and zigzag directions, which arises from the boundary scattering.
- <sup>27</sup>J. Callaway, *Phys. Rev.* **113**, 1046 (1959).
- <sup>28</sup>J. Shiomi and S. Maruyama, *Jpn. J. Appl. Phys.* **47**, 2005 (2008).
- <sup>29</sup>J. A. Thomas, R. M. Iutzi, and A. J. H. McGaughey, *Phys. Rev. B* **81**, 045413 (2010).